

A computational experimental of noise suppressing technique stand on hard decision threshold dissimilarity

Vorapoj Patanavijit¹, Kornkamol Thakulsukanant²

¹Department of Electrical and Electronic Engineering, Vincent Marry School of Engineering, Assumption University of Thailand, Bangkok, Thailand

²Department of Management Information Systems, Martin de Tours School of Management and Economics, Assumption University of Thailand, Bangkok, Thailand

Article Info

Article history:

Received Jun 2, 2021

Revised Aug 7, 2021

Accepted Aug 11, 2021

Keywords:

Digital image processing

Fixed-intensity impulse noise

Hard decision threshold dissimilarity

Noise suppressing techniques

ABSTRACT

Due to the extreme insistence for digital image processing, plentiful modern noise suppressing techniques are embodied of dissimilarity process and suppressing process. One of the extreme capability dissimilarity is hard decision threshold (HDT) dissimilarity, which has been recently declared in 2012, for suppressing the impulsive noisy photographs thus the computer experimental statement attempts to investigate the capability of the noise suppressing technique that is stand on HDT dissimilarity for the processed photographs, which are corrupted by fixed-intensity impulse noise (FIIN). This paper proposes the noise suppressing technique stand on HDT dissimilarity for FIIN. There are 3 primary contributions of this paper. The first contribution is the statistical average of the HDT dissimilarity of noise-free elements, which are computed from plentiful ground-truth photographs by varying window size for the best HDT window size. The second contribution is the statistical average of the HDT dissimilarity of corrupted elements, which are computed from plentiful corrupted photographs by varying outlier density for the best HDT window size. The final contribution is the statistical interrelation of the capability of the noise suppressing technique and hard consistent of HDT dissimilarity are investigated by varying the outlier denseness for the best HDT hard consistence.

This is an open access article under the [CC BY-SA](https://creativecommons.org/licenses/by-sa/4.0/) license.



Corresponding Author:

Vorapoj Patanavijit

Department of Electrical and Electronic Engineering

Vincent Marry School of Engineering, Assumption University of Thailand

PKE Bldg., 2nd Flr., 88 Moo 8 Bang Na-Trad Km. 26, Bangsaothong, Bangkok Thailand

Email: patanavijit@yahoo.com, patanavijit@gmail.com

1. LITURATURE REVIEW

Regularly, the competence of sophisticated image processing techniques [1]-[4], such as super resolution [5], remote sensing [6], and medical imaging [7]-[9], are definitely susceptible from noise thereupon noise suppressing technique [10]-[20] are become an irresistible momentous process. Theoretically, the noise suppressing technique regularly constructs the undesirable effect such as blurring effect or detail losing thereupon the fundamental intention of noise suppressing technique is for concealing noise from noisy photograph whereas protecting detail. Ordinarily, impulse noise [21]-[29] has a great impact to overall quality of the recorded photograph due to the fact that the impulse noise modifies the corrupted pixel element with irregular intensity. Naturally, photographs are corrupted by the impulse noise from plentiful reasons for instant transmission or receiver failure, overload of the circuit signal or etc. From mathematically analytical perspective, the impulse noise can be modeled into two kinds: random-intensity

impulse noise (RIIN), which can be varied from “0” to “255” and fixed-intensity impulse noise (FIIN), which can be either “0” or “255. For concealing an impulsive noise, specifically FIIN, the classic median filter (MF), which are originated by Pratt [21] in 1975, is readily implemented and has an acceptable competence thereupon MF has become the well-known noise suppressing technique nevertheless noise suppressing technique regularly constructs the undesirable effect such as great blurring effect or great detail losing because the MF deals with both noisy pixel elements and authentic pixel elements. Later, the noise suppressing technique stand on MF and adaptive window dimension for FIIN was originated by Hwang and Haddad [22] in 1994. Afterward, the noise suppressing technique stand on MF and detail-preserving regularization for FIIN was originated by Chan *et al.* [23] in 2005. Succeeding, the noise suppressing technique stand on statistical detection for RIIN was originated by Dong *et al.* [24] in 2007. Behind, the noise suppressing technique stand on probability existence detection for FIIN was originated by Awad [25] in 2018. Subsequently, the noise suppressing technique stand on inverse distance weighted interpolation (DBIDWI) for FIIN was investigated by Patanavijit [26] in 2019. Next, the noise suppressing technique stand on interpolation scheme for FIIN at high density was originated by Kishorebabu *et al.* [27] in 2019. Thereafter, the noise detection techniques stand on statistical analysis scheme for RIIN was investigated by Patanavijit and Thakulsukanant [28] in 2019. Later, the noise suppressing technique stand on multi-filters was investigated by Abdurrazzaq *et al.* [29] in 2019. As a results, plentiful noise suppressing techniques [21]-[32] have been modified from classic MF for only concealing impulsive noise pixels and un-touching noise-free pixels with better competence thereupon the hindrance of positioning identification of corrupted pixel elements is to identify the corrupted pixel element as noisy and identify the noise-free pixel element as noise-free. In order to separate the corrupted area from noise-free pixel element, the attribute of noise-free pixels, which are in smooth area (or almost all pixel intensity in this area are slightly equal) or in corner area (or all pixel intensity in this area are separated into two levels) nevertheless the almost area of pixels is smooth area but only few area of pixels is corner area. Ironically, the noisy pixels are great heterogeneity, which can be diffused from 0 to 255 due to impulsive noise thereupon noisy area has great heterogeneity of pixel intensity than the heterogeneity of noise-free area. As a results, the hard decision threshold (HDT) dissimilarity idea was originated by Awad [33] in 2012 for positioning identification of corrupted pixel elements and, later, was become one of the great competence dissimilarity for noisy/noise-free positioning identification that is incorporated in sophisticated noise suppressing technique. As consequence, the HDT dissimilarity was investigated during 0-100% density by [34]-[35] in 2020.

2. THE FUNDAMENTAL THEORY OF HDT DISSIMILARITY

The partition comprehensively prefaces the noise suppressing technique stand on both the positioning identification technique using HDT dissimilarity, which is assiduously elucidated in Section 2.1, and noise restoring technique using classical MF filter, which is assiduously elucidated in Section 2.2.

2.1. Positioning identification of impulse noise stand on HDT dissimilarity

Due to the algebra model of noisy images, which are corrupted by fix value impulsive outlier, the corrupted pixel element ($x(i, j)$) can be algebraically revealed as:

$$x(i, j) = \begin{cases} x_{noisy} & \text{if } x \in \bigcup_{i=1}^{i_0} \{C_i\} \text{ where } x_{noisy} \text{ and } x_{original} \text{ is noisy and original pixels} \\ x_{original} & \text{otherwise} \end{cases} \tag{1}$$

where C_i is the i^{th} noisy area and i_0 is the number of noisy area.

The HDT dissimilarity $d(i, j)$ [33] can be algebraically revealed as following technical expressions where the photograph size is defined as be $n \times m$, the window size is defined as $k \times l$, and the batch size is defined as $n' \times m'$.

$$d(i, j) = \sum_{s=k'}^{-k'} \sum_{t=l'}^{-l'} |y(s, t) - x(i, j)| \text{ where } k' = 0.5(k - 1) \text{ and } l' = 0.5(l - 1) \tag{2}$$

$$d(i, j) = \left| x(i, j) - \left(\frac{\sum_{s=k'}^{-k'} \sum_{t=l'}^{-l'} y(s, t)}{(k \times l)} \right) \right| \tag{3}$$

By varying the intensity of pixel element from 0” to “255” ($x(i, j) \in [0, 255]$), the simplification of the upper technical expressions can be algebraically revealed as:

$$\bar{y} = \left(\sum_{s=k'}^{k'} \sum_{t=l'}^{l'} y(s, t) \right) / (k \times l) = (b + a) / 2 = 255 / 2 \quad (4)$$

The HDT dissimilarity $d(i, j)$ at $x(i, j)$ is defined as:

$$d(i, j) = |(255/2) - x(i, j)| \quad (5)$$

The uncertain of the average of dissimilarities $d(i, j)$ can be algebraically revealed,

$$0 \leq d(i, j) \leq 127.5 \quad (6)$$

and

$$\bar{d}(i, j) = 63.75 \quad (7)$$

The average of dissimilarities D_c of the processed photograph can be algebraically revealed,

$$D_c = \left(\sum_{j=k'}^{n'-k'-1} \sum_{i=l'}^{m'-l'-1} d_c(i, j) \right) / ((n' - k' - 1) \times (m' - l' - 1)) \quad (8)$$

As a result of the computer computation results [33], the altering of regularized offset can be algebraically revealed,

$$D \leq Th \leq D_c \quad (9)$$

and

$$Th = (D + D_c) / 2 \quad (10)$$

The comprehensive processing of positioning identification of impulse noise stand on HDT dissimilarity can be algebraically revealed as Figure 1.

As a result of positioning identification processing for all pixel elements in the corrupted photograph, the corrupted pixel elements can be separated to be noise-free pixel elements or noisy pixel elements as,

$$x(i, j) = \begin{cases} x_{noisy} & \text{if } d(i, j) > Th \\ x_{original} & \text{otherwise} \end{cases} \quad (11)$$

2.2. Restoration of impulse noise stand on median filter

As a result of positioning identification processing for all pixel elements in the corrupted photograph, the corrupted pixel elements can be separated to be noise-free pixel elements or noisy pixel elements therefore only group of noisy pixel elements are suppressed as,

$$Med(i, j) = median \{ w(i-s, j-t) \bullet x(i-s, j-t) \mid -k' \leq s, t \leq k', (s, t) \neq (0, 0) \} \quad (12)$$

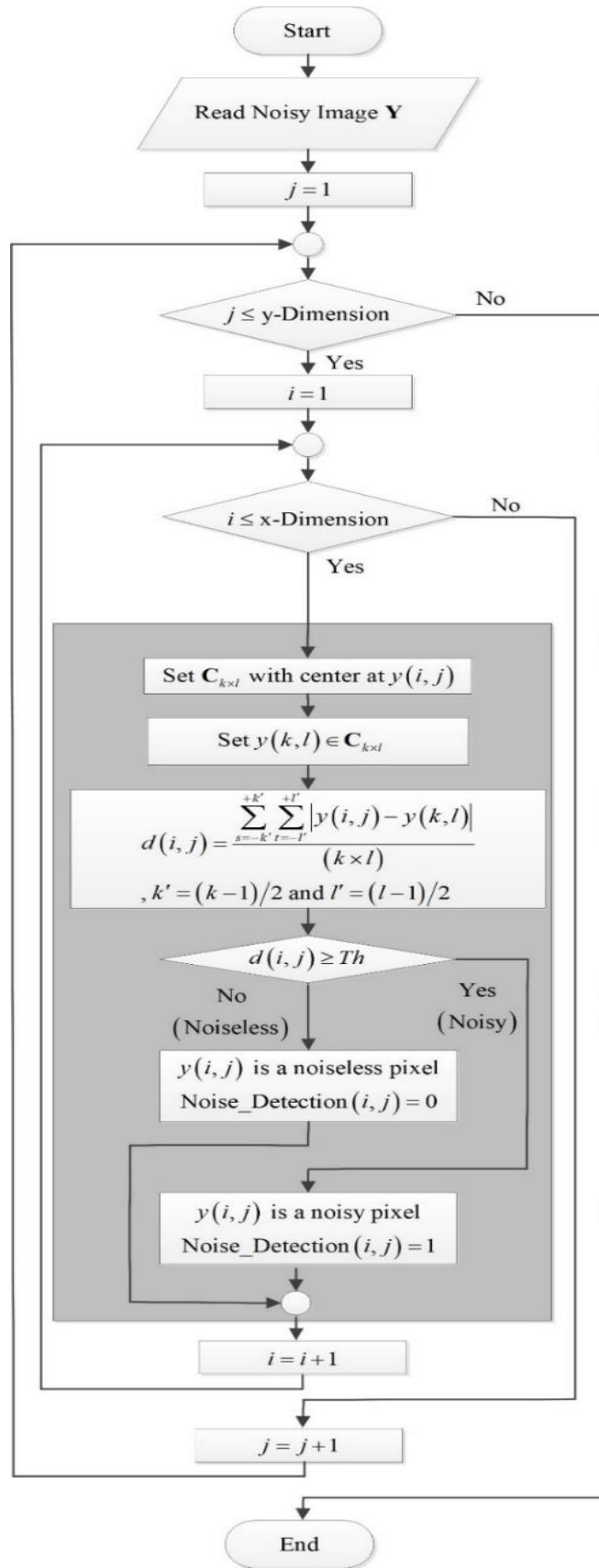


Figure 1. The comprehensive processing of positioning identification of impulse noise stand on HDT dissimilarity

3. THE LESSON OF THE COMPUTER CALCULATION OF NOISE SUPPRESSING TECHNIQUE STAND ON HDT DISSIMILARITY

The partition comprehensively prefaces the computer calculation of noise suppressing technique stand on HDT dissimilarity in two computer calculation lesson, which can be algebraically revealed as Figure 2 and Figure 3 for forcing the bibliophile the obvious perception on the computation process of noise suppressing technique stand on HDT dissimilarity in every computation step. The first calculation lesson can be algebraically revealed as Figure 2 where the processing pixel element $y_{i,j}$ is a noise-free pixel elements that is identified as noise-free by impulse noise identification process.

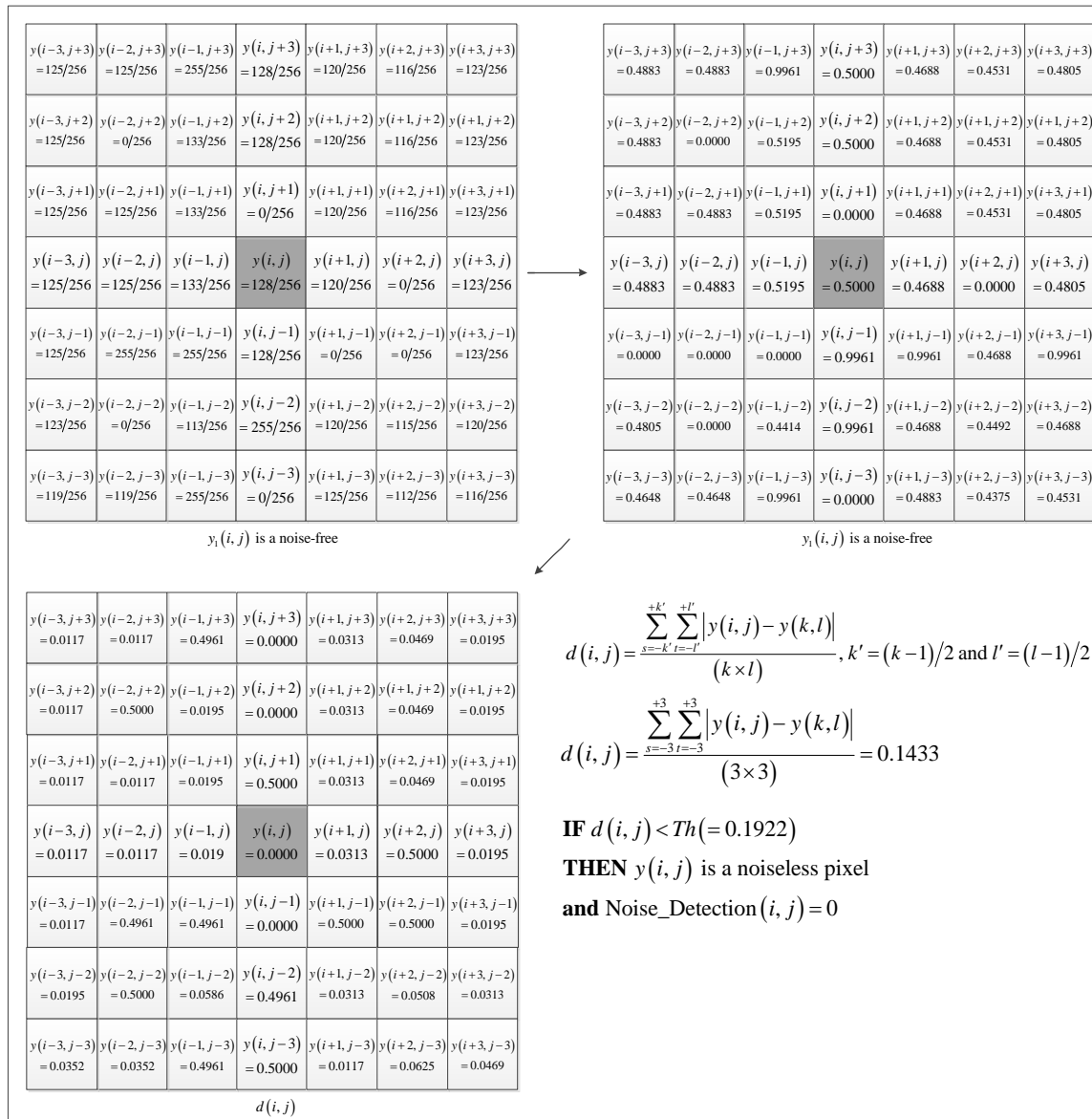


Figure 2. The first calculation lesson of noise suppressing technique stand on HDT dissimilarity (where the processing pixel element $y_{i,j}$ is a noise-free pixel elements)

Later, the calculation lesson can be algebraically revealed as Figure 2 where the processing pixel element $y_{i,j}$ is a noisy pixel elements that is identified as noise-free by impulse noise identification process and must be suppressed by impulse noise restoration process.

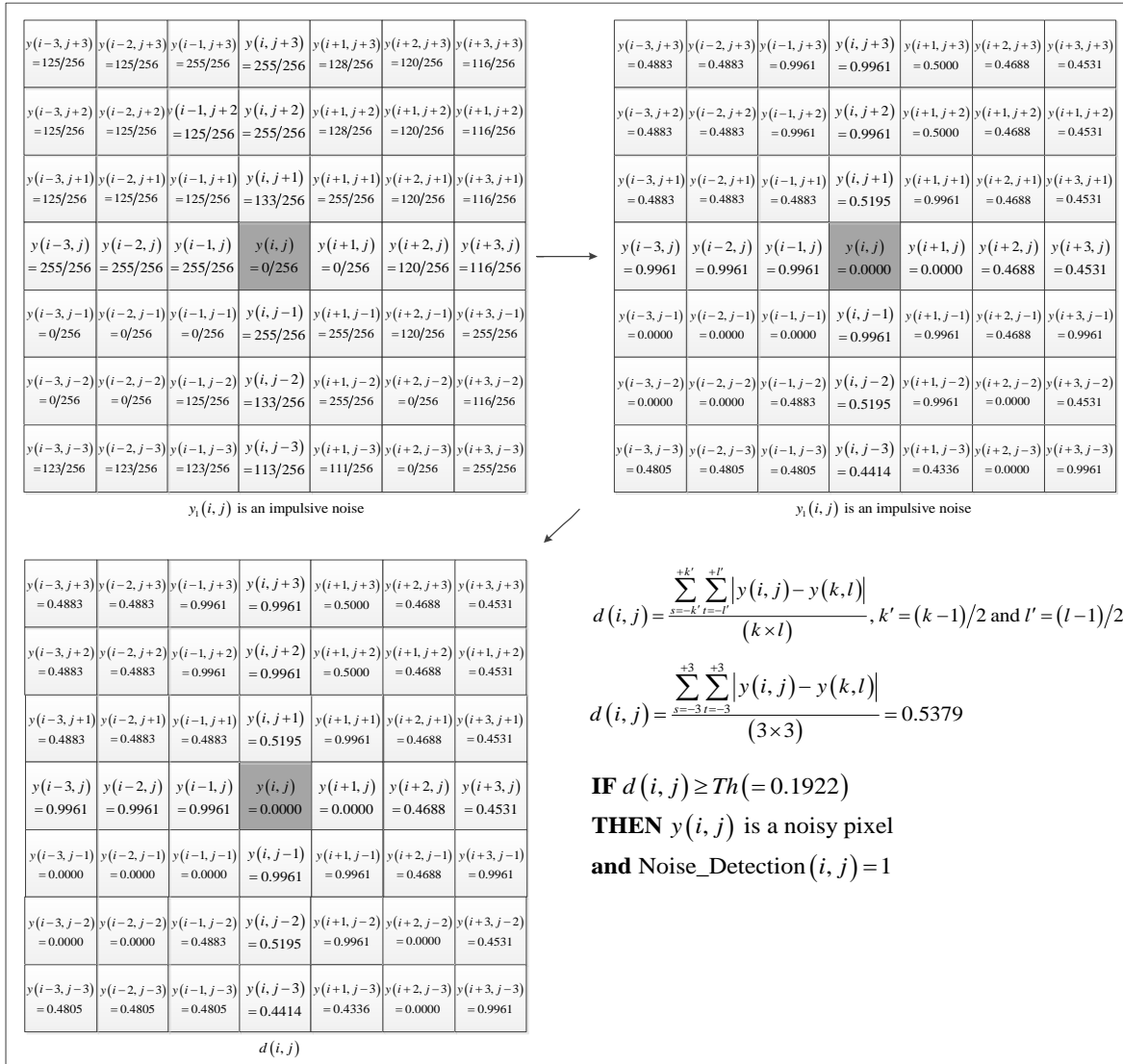


Figure 3. The first calculation lesson of noise suppressing technique stand on HDT dissimilarity (where the processing pixel element $y_{i,j}$ is a noisy pixel elements)

4. RESULTS AND DISCUSSION

In this partition of computer simulation, the simulation program is the MATLAB, which is installed and executed on plentiful workstations at this capability particularization: main processor i7-6700HQ and main executing memory 16 GB RAM. All workstations execute plentiful ground-truth photographs (which are compounded of Airplane, Baboon, Girl, House, Lena, Mobile, Pepper, Pentagon and Resolution) with bountiful noise frequency.

4.1. The computer simulation correlation of HDT dissimilarity and window dimension

From the results of computer simulation on plentiful ground-truth photographs, the first statistical moment and the second statistical moment of the normalized HDT dissimilarity of all ground-truth photographs (which are the noise-free photographs) are 0.0394 ± 0.0221 , 0.0506 ± 0.0275 and 0.0585 ± 0.0316 at window dimension 3×3 , 5×5 and 7×7 , respectively.

Next, the first statistical moment of normalized HDT dissimilarity $d(i, j)$ of all photographs, which are fluctuated from 0% to 90% noise frequency of FIIN at 3×3 , 5×5 and 7×7 could be laid out as Figure 4, Figure 5 and Figure 6, respectively. From these results of computer simulation, the normalized HDT dissimilarity with window dimension 7×7 provides the highest normalized absolute different. Consequently, the noise suppressing technique stand on HDT dissimilarity provides the highest peak signal to noise ratio (PSNR).

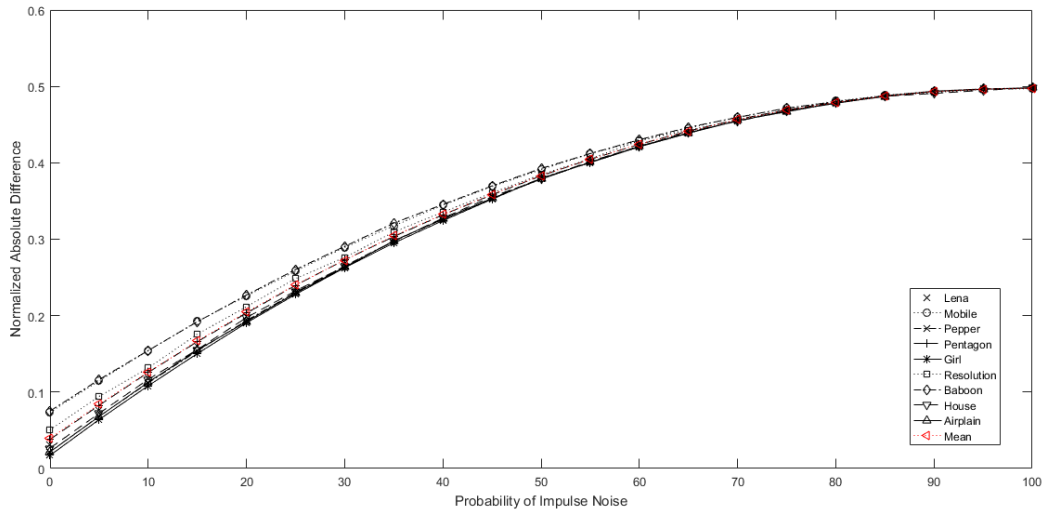


Figure 4. The computer simulation correlation of hdt dissimilarity at dimension 3x3 and noise density

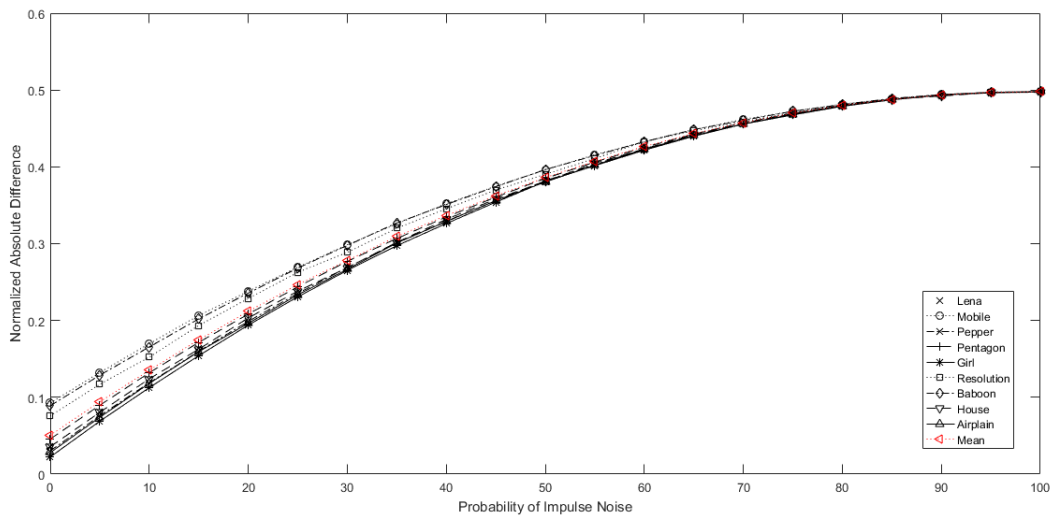


Figure 5. The computer simulation correlation of HDT dissimilarity at dimension 5x5 and noise density

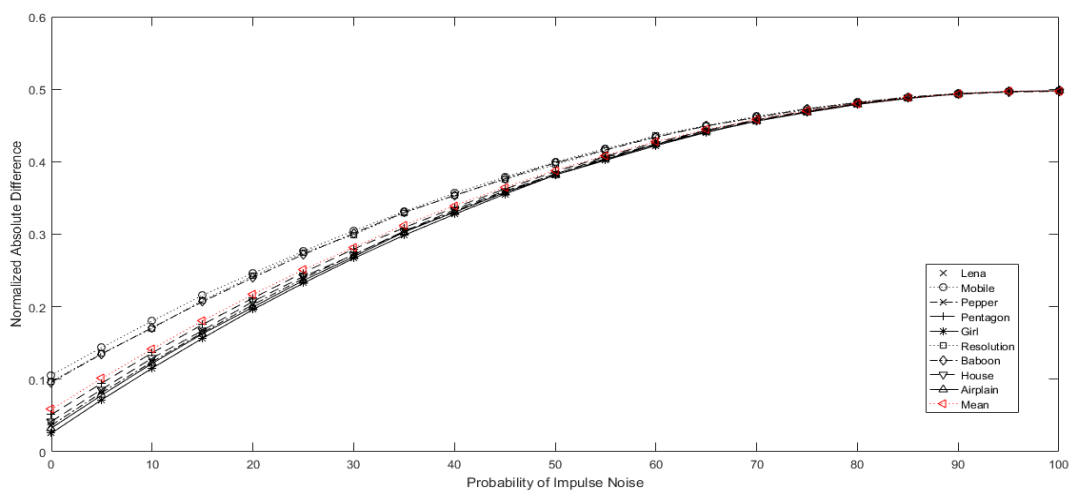


Figure 6. The computer simulation correlation of HDT dissimilarity at dimension 7x7 and noise density

4.2. The computer simulation correlation between noise suppressing capability and hard consistent of HDT dissimilarity

From the results of computer simulation on four ground-truth photographs, which are compounded of Girl, Lena, Airplane and Pepper, with the FIIN, the computer simulation correlation between noise suppressing capability and hard consistent of HDT dissimilarity could be laid out as Table 1, Table 2, Table 3 and Table 4, respectively (where the bold format is represented the highest PSNR). From the results of computer simulation consummations of Girl photographic, the HDT hard consistent for the most capability must be set during 0.025-0.375 roughly. By using algebraic investigation, the first statistical moment and the second statistical moment of the normalized HDT dissimilarity, which are calculated from these computer simulation consummations in Table 1, are 0.2417±0.1392. From the results of computer simulation consummations of Lena photographic, the HDT hard consistent for the most capability must be set during 0.025-0.350 roughly. By using algebraic investigation, the first statistical moment and the second statistical moment of the normalized HDT dissimilarity, which are calculated from these computer simulation consummations in Table 2, are 0.2278±0.1320.

Table 1. The computer simulation correlation of noise suppressing capability and hard consistent of HDT dissimilarity (Girl)

Hard Consistent	PSNR (dB)								
	10	20	30	40	50	60	70	80	90
0.025	34.69	31.90	27.69	23.37	20.17	18.45	16.73	16.11	12.64
0.050	30.71	31.27	27.64	23.37	20.17	18.45	16.73	16.11	12.64
0.075	28.12	29.43	27.45	23.39	20.18	18.45	16.73	16.11	12.64
0.100	26.82	27.86	27.01	23.36	20.17	18.45	16.73	16.11	12.64
0.125	26.89	27.01	26.56	23.35	20.19	18.45	16.73	16.11	12.64
0.150	27.43	26.96	26.10	23.70	20.23	18.48	16.74	16.11	12.64
0.175	28.28	27.24	26.22	24.05	20.41	18.56	16.75	16.11	12.64
0.200	29.13	27.96	26.42	24.73	20.87	18.79	16.77	16.11	12.64
0.225	29.88	28.64	27.18	25.29	21.77	19.27	16.83	16.13	12.63
0.250	30.28	28.94	27.62	26.10	23.08	19.87	16.94	16.14	12.63
0.275	30.12	28.91	27.74	26.55	24.61	21.17	17.42	16.24	12.60
0.300	29.55	28.20	27.46	26.77	25.42	22.40	18.30	16.42	12.50
0.325	29.24	27.46	26.68	26.37	25.67	23.58	19.43	16.61	12.23
0.350	29.33	27.01	26.04	25.55	25.21	23.97	20.71	16.77	11.45
0.375	29.53	26.85	25.49	24.79	24.37	23.66	21.40	16.56	10.17
0.400	29.63	26.89	25.16	24.17	23.66	22.81	21.33	16.10	9.19
0.425	29.59	26.85	24.95	23.75	23.07	22.14	20.74	15.68	8.81
0.450	29.57	26.77	24.80	23.50	22.63	21.30	19.57	15.24	8.80
0.475	29.51	26.73	24.76	23.25	22.19	20.54	18.11	13.92	8.46
0.500	29.51	26.67	24.67	23.07	21.74	19.48	16.44	12.09	7.56

Table 2. The computer simulation correlation of noise suppressing capability and hard consistent of HDT dissimilarity (Lena)

Hard Consistent	PSNR (dB)								
	10	20	30	40	50	60	70	80	90
0.025	34.73	32.15	27.91	23.79	20.57	18.17	17.12	16.38	14.17
0.050	31.40	31.98	27.91	23.79	20.57	18.17	17.12	16.38	14.17
0.075	27.99	31.07	27.90	23.79	20.57	18.17	17.12	16.38	14.17
0.100	26.48	28.79	27.74	23.79	20.57	18.17	17.12	16.38	14.17
0.125	26.15	26.87	27.30	23.82	20.58	18.17	17.12	16.38	14.17
0.150	26.91	25.87	26.37	23.99	20.58	18.17	17.12	16.38	14.17
0.175	28.29	26.30	25.59	24.13	20.66	18.18	17.12	16.38	14.17
0.200	29.79	27.27	25.71	24.58	20.94	18.19	17.12	16.38	14.17
0.225	31.24	28.66	26.43	24.93	21.65	18.25	17.08	16.35	14.16
0.250	32.46	29.79	27.53	25.47	22.79	18.56	17.07	16.31	14.13
0.275	32.31	30.13	28.24	26.36	23.67	19.47	17.01	16.11	14.00
0.300	31.13	29.24	28.19	26.79	24.64	20.73	17.08	15.46	13.70
0.325	29.37	27.50	26.98	26.21	24.86	21.83	17.25	14.35	12.60
0.350	28.06	25.62	25.08	24.49	23.77	22.18	17.47	13.13	10.92
0.375	26.52	23.93	22.98	22.59	22.02	21.21	17.75	11.89	9.24
0.400	25.20	22.54	21.19	20.73	19.88	19.29	17.08	11.85	7.96
0.425	24.13	21.34	19.68	18.91	17.91	17.04	15.60	12.25	7.78
0.450	23.16	20.10	18.42	17.22	16.12	15.06	13.84	11.83	8.53
0.475	22.14	19.07	17.26	15.82	14.59	13.32	12.26	10.75	8.79
0.500	21.25	18.05	16.19	14.66	13.32	11.93	10.93	9.66	8.28

From the results of computer simulation consummations of Airplane photographic, the HDT hard consistent for the most capability must be set during 0.025-0.350 roughly. By using algebraic investigation, the first statistical moment and the second statistical moment of the normalized HDT dissimilarity, which are calculated from these computer simulation consummations in Table 3, are 0.1778 ± 0.1308 . From the results of computer simulation consummations of Pepper photographic, the HDT hard consistent for the most capability must be set during 0.025-0.350 roughly. By using algebraic investigation, the first statistical moment and the second statistical moment of the normalized HDT dissimilarity, which are calculated from these computer simulation consummations in Table 4, are 0.1944 ± 0.1429 .

Table 3. The computer simulation correlation of noise suppressing capability and hard consistent of HDT dissimilarity (Airplane)

Hard Consistent	PSNR (dB)								
	10	20	30	40	50	60	70	80	90
0.025	34.15	31.38	27.13	23.01	19.62	17.66	16.25	15.64	13.89
0.050	30.96	31.20	27.12	23.01	19.62	17.66	16.25	15.64	13.89
0.075	27.72	29.95	27.07	23.01	19.62	17.66	16.25	15.64	13.89
0.100	26.10	27.77	27.04	23.03	19.62	17.66	16.25	15.64	13.89
0.125	25.89	26.39	26.80	23.07	19.62	17.66	16.25	15.64	13.89
0.150	26.34	25.55	25.73	23.41	19.64	17.66	16.25	15.64	13.89
0.175	26.82	25.59	24.97	23.87	19.80	17.67	16.25	15.64	13.89
0.200	27.23	25.98	25.03	24.15	20.24	17.73	16.24	15.64	13.89
0.225	27.20	26.17	25.39	24.10	21.17	17.96	16.25	15.63	13.89
0.250	27.04	25.93	25.16	24.11	22.00	18.47	16.24	15.60	13.84
0.275	27.10	25.37	24.68	23.82	22.73	19.45	16.36	15.45	13.77
0.300	27.10	24.87	24.04	23.32	22.88	20.43	16.70	15.03	13.60
0.325	26.88	24.40	23.29	22.66	22.50	21.14	17.46	14.49	12.98
0.350	26.48	24.01	22.60	21.93	21.76	21.03	18.00	13.87	11.63
0.375	26.03	23.40	21.93	21.17	20.81	20.27	17.79	13.06	10.14
0.400	25.50	22.91	21.30	20.46	19.83	19.29	17.53	13.02	8.85
0.425	25.16	22.47	20.72	19.77	18.93	18.16	16.79	13.03	8.44
0.450	24.84	22.10	20.22	19.17	18.15	17.07	15.51	12.81	8.86
0.475	24.58	21.70	19.77	18.59	17.37	16.08	14.14	11.94	8.90
0.500	24.32	21.36	19.41	18.02	16.65	14.97	12.79	10.84	8.33

Table 4. The computer simulation correlation of noise suppressing capability and hard consistent of HDT dissimilarity (Pepper)

Hard Consistent	PSNR (dB)								
	10	20	30	40	50	60	70	80	90
0.025	35.40	31.64	26.77	23.50	20.22	18.11	16.59	16.04	13.93
0.050	31.40	31.45	26.76	23.50	20.22	18.11	16.59	16.04	13.93
0.075	27.93	30.26	26.73	23.50	20.22	18.11	16.59	16.04	13.93
0.100	26.12	27.93	26.58	23.50	20.22	18.11	16.59	16.04	13.93
0.125	25.96	25.82	26.14	23.50	20.22	18.11	16.59	16.04	13.93
0.150	26.56	25.20	25.39	23.52	20.22	18.11	16.59	16.03	13.93
0.175	27.48	25.58	25.15	23.79	20.27	18.11	16.59	16.02	13.93
0.200	28.40	26.54	24.91	24.01	20.45	18.14	16.59	16.01	13.93
0.225	29.04	27.29	25.34	24.25	21.01	18.24	16.59	16.00	13.93
0.250	29.28	27.64	26.12	24.45	21.92	18.61	16.56	15.94	13.91
0.275	29.28	27.50	26.44	24.85	22.95	19.37	16.52	15.81	13.80
0.300	29.11	26.93	26.23	24.96	23.64	20.27	16.41	15.29	13.38
0.325	28.42	26.03	25.47	24.47	23.77	21.21	16.71	14.49	12.63
0.350	27.64	25.08	24.34	23.53	22.90	21.25	16.91	13.24	11.08
0.375	26.73	24.10	23.07	22.29	21.53	20.45	16.84	12.29	9.28
0.400	25.78	22.99	21.77	20.86	19.95	18.98	16.74	12.14	8.02
0.425	24.69	21.84	20.51	19.40	18.24	17.16	15.47	12.49	7.87
0.450	23.60	20.80	19.17	17.78	16.59	15.40	13.95	12.07	8.57
0.475	22.49	19.66	17.89	16.38	15.08	13.79	12.49	11.01	8.81
0.500	21.60	18.50	16.75	15.15	13.81	12.55	11.21	9.91	8.33

4.3. The comprehensive capability of the noise suppressive technique stand on HDT dissimilarity

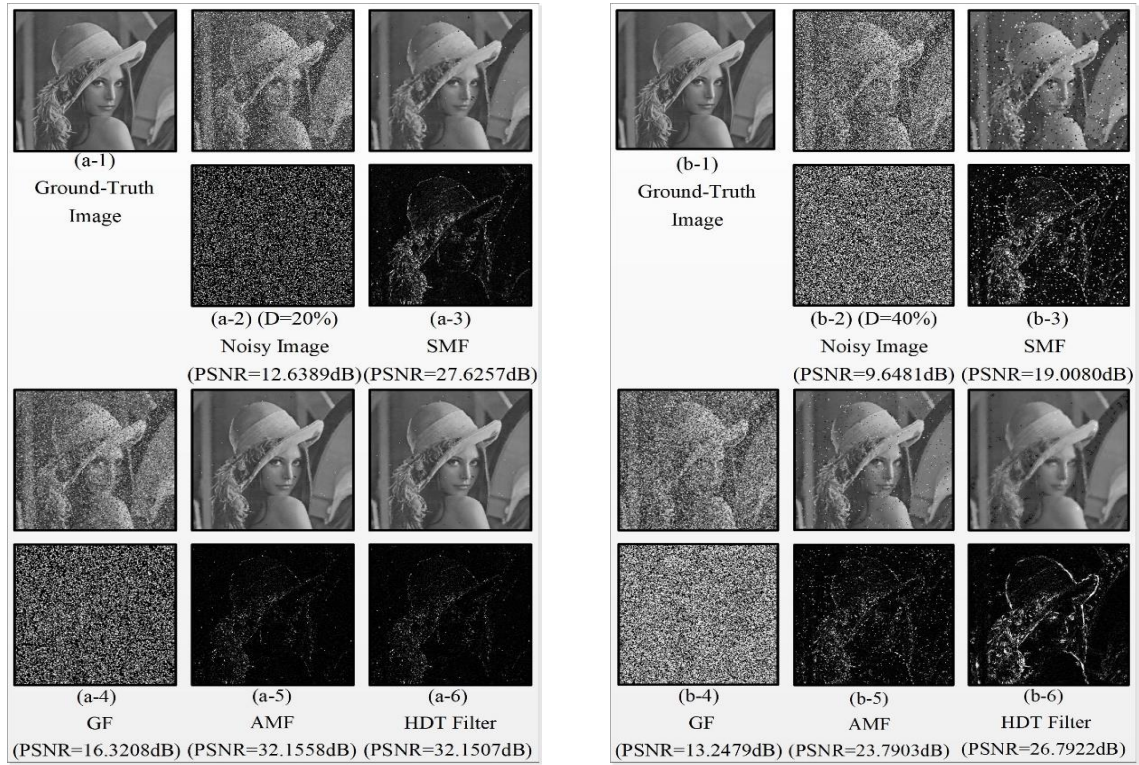
In consideration of the PSNR capability of the noise suppressing technique stand on HDT dissimilarity, the experimental simulation of the noise suppressive technique stand on HDT dissimilarity with the optimized HDT hard consistent, which are investigated from the previous simulation, are investigated on four ground-truth photographs (Girl, Lena, Airplane and Pepper) by corrupting FIIN at plentiful frequency

during 0% to 90% and are compared to MF, smoothing filter (SF) and adaptive median filter (AMF), which could be laid out as Table 5. From the results of computer simulation consummations of four photographs in Table 5, the noise suppressing technique stand on HDT dissimilarity is superb than all other noise suppressing techniques because the impulsive noise positioning identification stand on HDT dissimilarity is very high accuracy thus the noise suppressing technique stand on HDT dissimilarity only conceals impulsive noise pixels and un-touches noise-free pixels.

By cause of the publication circumspection of pages, the partition of a computational experimental investigation provides few suppressed photographs, which are processed by MF, SF, AMF and HDT, which could be laid out as Figure 7. From the results in Figure 7, the quality of the HDT suppressed images are slightly better than AMF suppressed images and dramatical better than MF and SF suppressed images.

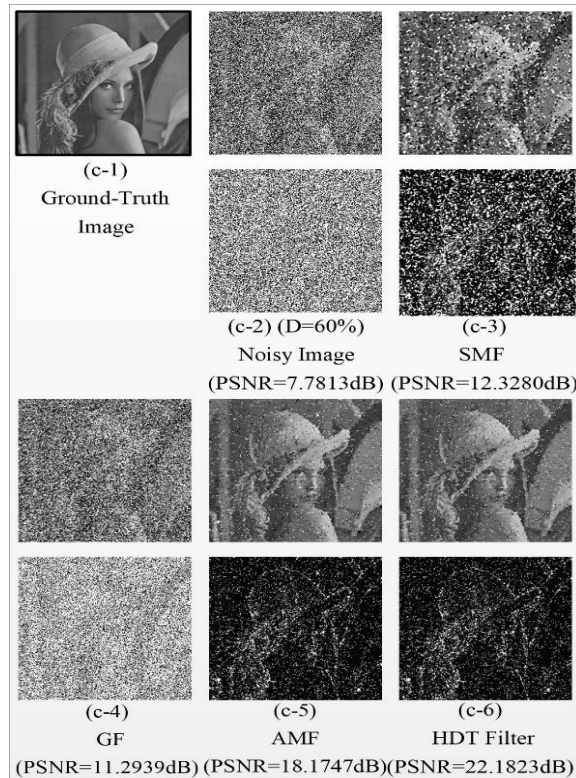
Table 5. The computer simulation correlation of noise suppressing capability and hard consistent of HDT dissimilarity (pepper)

Processed Photographs	PSNR (dB)					
	Noise Frequency	Noisy Photo graphs	Noise Suppressing Technique			
			SMF (3x3)	SF (3x3)	AMF	HDT Filter
Lena (256x256)	D=0.10	15.6564	30.7076	19.3812	35.3032	34.7294
	D=0.20	12.6389	27.6257	16.3208	32.1558	32.1507
	D=0.30	10.8971	23.6811	14.5829	27.9141	28.2383
	D=0.40	9.6481	19.0080	13.2479	23.7903	26.7922
	D=0.50	8.6553	15.4758	12.2146	20.5725	24.8559
	D=0.60	7.7813	12.3280	11.2939	18.1747	22.1823
	D=0.70	7.1697	10.2861	10.6509	17.1153	17.7479
	D=0.80	6.5846	8.3331	10.0057	16.4554	16.3753
	D=0.90	6.0604	6.8241	9.4356	16.5352	14.1720
	D=1.00	15.3798	30.6116	19.0677	36.0391	35.4041
Pepper (256x256)	D=0.10	12.3593	26.5888	15.9804	31.6485	31.6440
	D=0.20	10.6242	22.0663	14.1748	26.7650	26.7650
	D=0.30	9.3998	18.4321	12.9076	23.4995	24.9567
	D=0.40	8.3843	14.8506	11.8117	20.2203	23.7720
	D=0.50	7.6189	12.0128	10.9563	18.1116	21.2489
	D=0.60	6.9246	9.7704	10.2039	16.5923	16.9106
	D=0.70	6.3710	8.0166	9.5853	16.0896	16.0352
	D=0.80	5.8582	6.5767	9.0214	16.2932	13.9343
	D=0.90	14.8320	29.6532	18.4426	34.6311	34.1514
	D=1.00	11.8045	26.4356	15.3181	31.3844	31.3782
Airplane (256x256)	D=0.10	10.0510	21.8862	13.4526	27.1347	27.1346
	D=0.20	8.8735	17.6412	12.1397	23.0147	24.1547
	D=0.30	7.8600	14.2697	11.0091	19.6201	22.8765
	D=0.40	7.0920	11.5290	10.1202	17.6586	21.1398
	D=0.50	6.4128	9.3042	9.3238	16.2514	18.0006
	D=0.60	5.8647	7.5835	8.6893	15.7428	15.6423
	D=0.70	5.3335	6.0278	8.0381	16.0834	13.8896
	D=0.80	13.6890	31.5583	17.2530	36.9197	34.6863
	D=0.90	10.6567	25.5153	13.9593	32.0437	31.8964
	D=1.00	8.8677	20.7738	11.9599	27.6930	27.7366
Girl (256x256)	D=0.10	7.5798	16.5146	10.4543	23.3736	26.7717
	D=0.20	6.5712	13.0319	9.2367	20.1712	25.6672
	D=0.30	5.8609	10.4981	8.3590	18.4518	23.9741
	D=0.40	5.1311	8.0463	7.4271	16.7334	21.3971
	D=0.50	4.5674	6.2520	6.6881	16.2795	16.7662
	D=0.60	4.0573	4.7465	5.9986	16.7463	12.6371
	D=0.70					
	D=0.80					
	D=0.90					
	D=1.00					



(a)

(b)



(c)

Figure 7. (a). The computer simulation correlation of HDT dissimilarity at 7x7 at dimension 7x7 and noise density (LENA at 20% noise density), (b). The computer simulation correlation of HDT dissimilarity at 7x7 at dimension 7x7 and noise density (LENA at 40% noise density), (c). The computer simulation correlation of HDT dissimilarity at 7x7 at dimension 7x7 and noise density (LENA at 60% noise density)

5. CONCLUSION

The computer experimental statement attempts to investigate the capability of the noise suppressing technique that is stand on HDT dissimilarity for the processed photographs, which are corrupted by fix intensity impulsive noise. The first contribution is the determination of the best window size of the HDT dissimilarity from plentiful photographs by varying window size from 3x3 to 7x7 for the outlier denseness from 0% to 100%. The second contribution is the determination of the optimized hard consistent of HDT dissimilarity for the highest capability for the outlier denseness from 0% to 90%. The final contribution is the determination of the capability of the noise suppressing technique based the optimized hard consistent of HDT dissimilarity for the outlier denseness from 0% to 90% for FIIN.

REFERENCES

- [1] R. C. Gonzalez and R. E. Woods, "Digital Image Processing, Prentice-Hall, Upper Saddle River," *NJ, USA, 2nd edition*, 2002, doi: 10.5406/ethnomusicology.55.2.0336.
- [2] M. M. Rahman and A. S. M. Shafi, "Decomposition of color wavelet with higher order statistical texture and convolutional neural network features set based classification of colorectal polyps from video endoscopy," *International Journal of Electrical and Computer Engineering (IJECE)*, vol. 10, no. 3, pp. 2986-2996, June 2020, doi: 10.11591/ijece.v10i3.pp2986-2996.
- [3] S. Bagchi, A. Huang, S. K. Debnath, and T. K. Gaik, "Image processing and machine learning techniques used in computer-aided detection system for mammogram screening-A review," *International Journal of Electrical and Computer Engineering (IJECE)*, vol. 10, no. 3, pp. 2336-2348, June 2020, doi: 10.11591/ijece.v10i3.pp2336-2348.
- [4] G. César Pachón-Suescún, and C. J. Enciso-Aragón, "Robotic navigation algorithm with machine vision," *International Journal of Electrical and Computer Engineering (IJECE)*, vol. 10, no. 2, pp. 1308-1316, April 2020, doi: 10.11591/ijece.v10i2.pp1308-1316.
- [5] D. Kesrarat, K. Thakulsukanant, and V. Patanavijit, "A Novel Elementary Spatial Expanding Scheme Form on SISR Method with Modifying Geman&Mcclure Function," *TELKOMNIKA (Telecommunication Computing Electronics and Control)*, vol. 17, no. 5, pp. 2554-2560, Oct 2019, doi: 10.12928/telkomnika.v17i5.12799.
- [6] S. Ahmed Mir, and T. Padma, "Satellite Image Denoising Using Discrete Cosine Transform," *Indonesian Journal of Electrical Engineering and Informatics (IJEI)*, vol. 5, no. 4, pp. 372-375, December 2017, doi: 10.11591/ijece.v5i4.369.
- [7] A. M. Hasan, "A Hybrid Approach of Using Particle Swarm Optimization and Volumetric Active Contour without Edge for Segmenting Brain Tumors in MRI Scan," *Indonesian Journal of Electrical Engineering and Informatics (IJEI)*, vol. 6, no. 3, pp. 292-300, September 2018, doi: 10.11591/ijece.v6i3.592.
- [8] N. Hammouch, and H. Ammor, "A confocal microwave imaging implementation for breast cancer detection," *Indonesian Journal of Electrical Engineering and Informatics (IJEI)*, vol. 7, no. 2, pp. 263-270, June 2019, doi: 10.11591/ijece.v7i2.806.
- [9] C. Bhardwaj, S. Jain, and M. Sood, "Automatic Blood Vessel Extraction of Fundus Images Employing Fuzzy Approach," *Indonesian Journal of Electrical Engineering and Informatics (IJEI)*, vol. 7, no. 4, pp. 757-771, Dec 2019, doi: 10.11591/ijece.v7i4.991.
- [10] V. Patanavijit, "The Bilateral Denoising Performance Influence of Window," *Spatial and Radiometric Variance, ICAICTA2015*, 2015, doi: 10.1109/ICAICTA.2015.7335350.
- [11] O. Prakash Verma and N. Sharma, "Intensity Preserving Cast Removal in Color Images Using Particle Swarm Optimization," *International Journal of Electrical and Computer Engineering (IJECE)*, vol. 7, no. 5, pp. 2581-2595, October 2017, doi: 10.11591/ijece.v7i5.pp2581-2595.
- [12] M. Hamiane and F. Saeed, "SVM Classification of MRI Brain Images for Computer-Assisted Diagnosis," *International Journal of Electrical and Computer Engineering (IJECE)*, vol. 7, no. 5, pp. 2555-2564, October 2017, doi: 10.11591/ijece.v7i5.pp2555-2564.
- [13] A. Khmag, S. Ghoul, and S. Abdul Rahman Al-Haddad, "Noise Level Estimation for Digital Images Using Local Statistics and Its Applications to Noise Removal," *TELKOMNIKA (Telecommunication Computing Electronics and Control)*, vol. 16, no. 2, pp. 915-924, April 2018, doi: 10.12928/telkomnika.v16i4.9060.
- [14] K. Arun Sai, and K. Ravi, "An Efficient Filtering Technique for Denoising Colour Images," *International Journal of Electrical and Computer Engineering (IJECE)*, vol. 8, no. 5, pp. 3604-3608, October 2018, doi: 10.11591/ijece.v8i5.pp3604-3608.
- [15] Z. M. Ramadan, "Effect of kernel size on Wiener and Gaussian image filtering," *TELKOMNIKA (Telecommunication Computing Electronics and Control)*, Indonesia, vol. 17, no. 3, pp. 1455-1460, June 2019, doi: 10.12928/TELKOMNIKA.v17i3.11192.
- [16] R. Syelly, A. Ramadhanu, J. Naam, and J. Harlan "Filter technique of medical image on multiple morphological gradient (MMG) method," *TELKOMNIKA (Telecommunication Computing Electronics and Control)*, vol. 17, no. 3, pp. 1317-1323, June 2019, doi: 10.12928/telkomnika.v17i1.9722.
- [17] B. Charmouti, A. K. Junoh, M. Y. Mashor, N. Ghazali, and M. Ab Wahab "An overview of the fundamental approaches that yield several image denoising techniques," *TELKOMNIKA (Telecommunication Computing Electronics and Control)*, vol. 17, no. 6, December 2019, doi: 10.12928/telkomnika.v17i6.11301.
- [18] B. Charmouti, A. K. Junoh, M. Y. Mashor, N. Ghazali, and M. Ab Wahab "Progression approach for image denoising," *TELKOMNIKA (Telecommunication Computing Electronics and Control)*, vol. 17, no. 6, pp. 29948-2958, December 2019, doi: 10.12928/telkomnika.v17i6.12408.

- [19] A. Jeelani, M. B. Veena, "Denoising using Self Adaptive Radial Basis Function," *Indonesian Journal of Electrical Engineering and Informatics (IJEI)*, vol. 7, no. 4, pp. 677-685, Dec 2019, doi: 10.11591/ijeii.v7i4.948.
- [20] Y. Y. Al-Aboosi, R. S. Issa, and A. K. Jassim "Image denosing in underwater acoustic noise using discrete wavelet transform with different noise level estimation," *TELKOMNIKA (Telecommunication Computing Electronics and Control)*, vol. 18, no. 3, pp. 1439-1446, June 2020, doi: 10.12928/TELKOMNIKA.v18i3.14381.
- [21] W. K. Pratt, "Median filtering," *Tech. Rep., Image Proc. Inst.*, Univ. Southern California, Los Angeles, Sep. 1975.
- [22] H. Hwang and R. A. Haddad, "Adaptive median filters: new algorithms and results," in *IEEE Transactions on Image Processing*, vol. 4, no. 4, pp. 499-502, April 1995, doi: 10.1109/83.370679.
- [23] R. H. Chan, C. W. Ho and M. Nikolova, "Salt-and-pepper noise removal by median-type noise detectors and detail-preserving regularization," in *IEEE Transactions on Image Processing*, vol. 14, no. 10, pp. 1479-1485, Oct. 2005, doi: 10.1109/TIP.2005.852196.
- [24] Y. Dong, R. H. Chan, and S. Xu, "A Detection Statistic for Random-Valued Impulse Noise," in *IEEE Transactions on Image Processing*, vol. 16, no. 4, pp. 1112-1120, April 2007, doi: 10.1109/TIP.2006.891348.
- [25] A. Awad, "Removal of Fixed-valued Impulse Noise based on Probability of Existence of the Image Pixel," *International Journal of Electrical and Computer Engineering (IJECE)*, vol. 8, no. 4, pp. 2106-2114, August 2018, doi: 10.11591/ijece.v8i4.pp2106-2114.
- [26] V. Patanavijit, "Denoising Performance Analysis of Adaptive Decision Based Inverse Distance Weighted Interpolation (DBIDWI) Algorithm for Salt and Pepper Noise," *Indonesian Journal of Electrical Engineering and Computer Science (IJECS)*, vol. 15, no. 2, pp. 804-813, Aug. 2019, doi: 10.11591/ijeecs.v15.i2.pp804-813.
- [27] V. Kishorebabu, G. Packyanathan, H. Kamatham, and V. Shankar, "An adaptive decision based interpolation scheme for the removal of high density salt and pepper noise in images," *EURASIP Journal on Image and Video Processing*, vol. 1, pp. 1-18, 2017, doi: 10.1186/s13640-017-0215-0.
- [28] V. Patanavijit and K. Thakulsukanant, "The Statistical Analysis of Random-Valued Impulse Noise Detection Techniques Based on The Local Image Characteristic: ROAD, ROLD and RORD," *Indonesian Journal of Electrical Engineering and Computer Science (IJECS)*, vol. 15, no. 2, pp. 794-803, Aug. 2019, doi: 10.11591/ijeecs.v15.i2.pp794-803.
- [29] A. Abdurrazzaq, A. K. Junoh, W. Z. Azman Wan Muhamad, Z. Yahya, and I. Mohd, "An overview of multi-filters for eliminating impulse noise for digital images," *TELKOMNIKA (Telecommunication Computing Electronics and Control)*, vol. 17, no. 6, pp. 385-393, December 2019, doi: 10.12928/telkomnika.v18i1.12888.
- [30] S. M. Helmi, M. F. M. Jusof, and M. A. Ahmad, "Dual Sliding Statistics Switching Median Filter for the Removal of Low Level Random-Valued Impulse Noise," *Journal of Electrical Engineering and Technology*, vol. 13, no. 3, pp. 1383-1391, 2018, doi: 10.5370/JEET.2018.13.3.1383.
- [31] T. Veerakumar, B. N. Subudhi, and S. Esakkirajan, "Empirical mode decomposition and adaptive bilateral filter approach for impulse noise removal," *Expert Systems with Applications*, vol. 121, pp. 18-27, 2019, doi: 10.1016/j.eswa.2018.12.009.
- [32] S. Khan and D. H. Lee, "An adaptive dynamically weighted median filter for impulse noise removal," *EURASIP Journal on Advances in Signal Processing*, vol. 1, pp. 1-14, 2017, doi: 10.1186/s13634-017-0502-z.
- [33] A. S Awad, "Localizing and restoring clusters of impulse noise based on the dissimilarity among the image pixels," *EURASIP Journal on Advances in Signal Processing*, vol. 1, pp. 1-7, 2012, doi: 10.1186/1687-6180-2012-161.
- [34] V. Patanavijit and K. Thakulsukanant, "A Comprehensive Statistical Scrutiny of HDT Dissimilarity for Localizing and Restoring Impulsive Noisy Images," *Proceeding of The 17th Annual International Conference of Electrical Engineering/Electronics, Computer, Telecommunications and Information Technology (ECTI-CON 2020)*, ECTI Association Thailand, Phuket, Thailand, June 2020, doi: 10.1109/ECTI-CON49241.2020.9158124.
- [35] D. Kesrara, K. Thakulsukanant, and V. Patanavijit, "An Extensive Demographic Inquiry of HDT Distinction for Localizing and Reestablishing Impulsive Irregularity Illustrations," *The 2021 International Conference on Power, Energy and Innovations (ICPEI2021)*, Nakhon Ratchasima, Thailand, Oct. 2021, doi: 10.1109/ECTI-CON49241.2020.9158124.